

Ship hull flexure measurement based on integrated GNSS/LINS

Di WU^{1,2}, Yu JIA (✉)³, Li WANG³, Yueqiang SUN¹

¹ National Space Science Center, Chinese Academy of Sciences, Beijing 100190, China

² University of Academy of Sciences, Beijing 100049, China

³ Huazhong Institute of Electro-optics—Wuhan National Laboratory for Optoelectronics, Wuhan 430223, China

© Higher Education Press and Springer-Verlag GmbH Germany, part of Springer Nature 2019

Abstract For precision carrier-based landing aid, the position of reference point on the top of island shall be precisely transferred to the landing point on the deck, so the position transfer error caused by the hull flexure is not negligible. As the existing method is not very applicable to measure the hull flexure, a new technique based on integrated Global Navigation Satellite Systems/Laser Gyro Inertial Navigation System (GNSS/LINS) is proposed in this paper. This integrated GNSS/LINS based measurement method is designed to monitor the hull flexure and set up an integrated GNSS/LINS measurement model based on raw pseudo-range and pseudo-range rate measurement and carrier phase differential positioning measurement to effectively eliminate the measurement error caused by cycle slip and multi-path effect from GNSS. It is shown by demonstration test and analysis that this technique has the capability to precisely measure the hull flexure, with the accuracy being better than 0.02 m.

Keywords satellite navigation, inertial navigation, flexure measurement, Laser Gyro

1 Introduction

Precision differential positioning technique based on satellite navigation is used for carrier-based aircraft landing aid to guide the aircrafts for precise landing and realize relatively positioning of carrier ship base and carrier aircraft. On the carrier ship, the differential positioning reference point is located at the phase center of receiver antenna while the landing point is located on the cross area of central line of deck and the 2nd and 3rd arresting wire.

To avoid satellite signal above the deck to be blocked and eliminate the multi-path effect, the receiver antenna shall be installed up on a mast of the carrier ship. However, the baseline between antenna reference point and landing point shall vary with the carrier attitude and hull flexural deflection in real time [1,2], therefore the flexure variation between antenna reference point and landing point shall be precisely measured.

Now the method to precisely measure the hull flexure includes: optical measurement method (i.e., optical two frequency polarization [3], self-collimation parallel light method [4], laser tracking method [5] and photographing method [6]), satellite navigation based differential positioning measurement method [7] and inertial match measurement method [8]. The optical measurement method features high accuracy and high fidelity, but has the disadvantage of low adaptability and flexibility owing to demanding a non-breaking optical path between different observation points. As for the satellite navigation based differential positioning method, it is difficult to eliminate cycle-slip and multi-path effect. Moreover, the update frequency of flexure information measured by hull cannot be over 100 Hz [7]. As for the inertial match measurement method, the sensitivity of Kalman filter and estimation of flexure are constraints for its application in hull flexure measurement [8].

In this paper, an integrated Global Navigation Satellite Systems/Laser Gyro Inertial Navigation System (GNSS/LINS) method is proposed to realize precise measurement of ship hull flexure, featuring low noise, high frequency and high precision. GNSS shall be able to provide precise positioning data, and its measurement error does not accumulate with time, but its sampling frequency is low, and susceptible to environment interference. The laser gyroscope features good scale factor linearity, high stability, minor dynamic environment error, anti-vibration, anti-shock and environment adaptability, so it is applicable

for hull flexure monitoring in adverse environment, providing high accuracy high frequency angular measurement result, but negatively with fast accumulating measurement error with time. Therefore, integrated GNSS/LINS measurement can learn from the other's strong point to offset one's weakness to improve the overall performance. As the two ends of baseline for flexure monitoring are both fused with high rate sampling and high accuracy inertial navigation information, flexure error, inertial unit error and satellite navigation receiver clock error can be modeled for high precision estimation.

2 Measurement method of integrated GNSS/LINS

The measurement error of laser gyroscope plays a decisive role in hull flexure measurement. It shall be able to decrease the gyroscope bias and angle random wandering noise to effectively improve the flexure measurement accuracy [9]. As the laser gyroscope is based on Sagnac effect, it measures the optical path difference of two-way beams in the resonant cavity to work out the angle variation and effectively reduce the gyroscope measurement noise by improving the optical manufacturing quality of resonant cavity. As for the laser gyroscope used in our test, the optical process is improved by means as followed.

1) Use super-smooth polishing technique in large curvature radius to make the lens roughness to be lower than 1 \AA ;

2) Use double ion beam sputter (DIBS) coating technique to make the backscattering up to be 5×10^{-6} , without any flaw;

3) The optical cavity of laser gyroscope shall be precisely manufactured in a high precision optical manufacturing center and polished by classical technique to make the angular error of each critical surface up to be second of arc.

Through the above optical process improvement approaches, the laser gyroscope measurement bias stability is better than 0.003 deg/h , and the random wandering noise is better than $0.0008 \text{ deg/sqrt(h)}$.

As shown in Fig. 1, the measured baseline of the ship flexure is consisting of the landing point and the differential positioning reference point. Two sets of integrated GNSS/LINS unit shall be installed at the measured baseline of the ship, which mainly composed of LINS, satellite receiver and receiver antenna. One of the satellite antenna and LINS are installed in the position of differential positioning reference point on the mast; the other antenna is installed on the edge of deck and the LINS shall be installed inside the deck of landing point. Integrated GNSS/LINS flexure measurement technique is to calculate and compensate the inertial navigation error, satellite navigation clock error and baseline resolving error. The work procedure of integrated GNSS/LINS method is as follows.

1) Combine and resolve the pseudo-range and pseudo-range rate obtained by the satellite navigation receiver and LINS at two ends. Take the difference between pseudo-range obtained by the satellite navigation receiver and pseudo-range predicted by the LINS to refresh the Kalman filter, so as to precisely calculate and compensate the inertial navigation error and satellite navigation receiver clock error.

Tight integration GNSS/LINS method is designed to

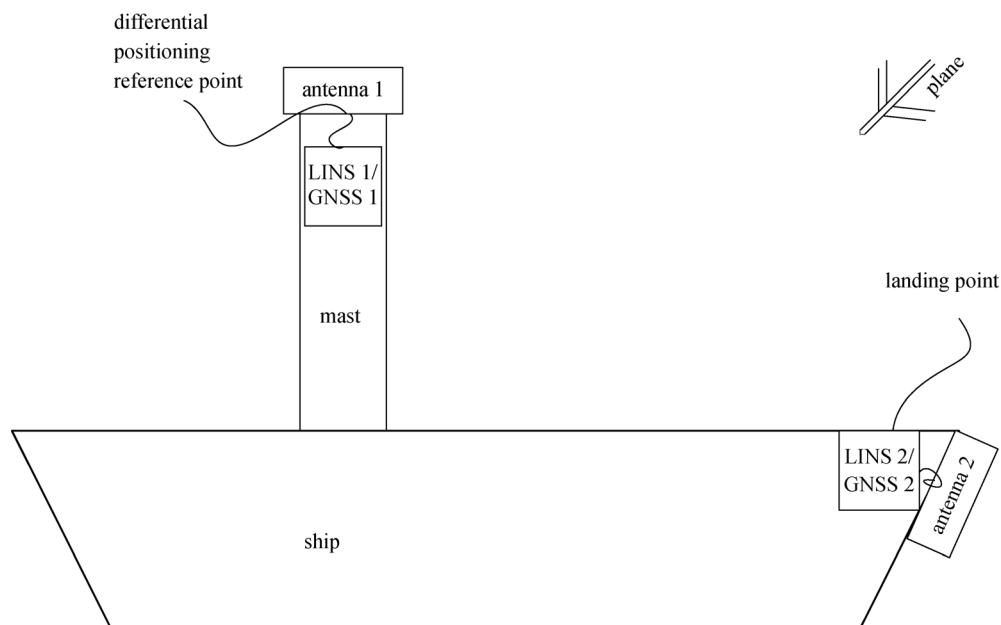


Fig. 1 Integrated GNSS/LINS schematic diagram

carry out optimal estimation of position, velocity, altitude and sensor zero deviation of navigation system by using the Kalman filter and correct the inertial navigation output according to the estimated result [7]. The Kalman filter shall take the pseudo-range and pseudo-range rate obtained from GNSS to be observation vector input and, in combination with LINS output and satellite ephemeris to predict the pseudo-range and pseudo-range and take the difference between measured value and predicted value. Then the measured value shall be sent to the Kalman filter for estimation of correction value of each state parameter, with the covariance matrix of initial state parameters, noise covariance matrix of state equation and covariance matrix of observation noise to be given. The resolved correction value shall be then sent back the LINS mechanization to suppress the accumulative error of LINS [9]. Block diagram of tight integration GNSS/LINS is shown in Fig. 2.

2) The phase-derived result obtained by the satellite navigation receiver shall be used to resolve as a baseline in real time directly using carrier phase differential positioning method. Take the difference between the resolved baseline and the baseline predicted by LINS at two ends and use this difference to refresh the state vector of Kalman filter to precisely calculate the inertial navigation error, relative baseline position and position variation.

2.1 Kalman filtering modeling

Kalman filtering model [10] is used in integrated GNSS/LINS measurement method. The LINS data shall be synchronized with the pseudo-range and pseudo-range rate obtained from GNSS receiver and then sent to the Kalman filter for combination processing (a tight integration algorithm). The inertial navigation state error shall quickly be accumulated with time and the Intertial Measure Unit (IMU) error also shall quickly vary with time, so, by means of Kalman filtering, the LINS error shall be estimated and corrected on line according to the measurement data from

GNSS. In the process of modeling for tight integration GNSS/LINS algorithm, the corresponding state equation and observation equation shall be set up, in which the LINS dynamic error model shall correspond to the state equation while the GNSS error model shall correspond to the observation equation. The observation components of observation equation shall include two parts: one is the difference between pseudo-range and pseudo-range rate predicted according to LINS position, velocity and satellite ephemeris and pseudo-range and pseudo-range rate observed by GNSS, and the other is the difference between baseline vector resolved by carrier phase differential positioning at two ends of baseline and baseline vector resolved by integrated LINS at two ends.

2.2 Error state model

As the LINS mechanization will take the local horizontal coordinate system (east-north-up direction) to be reference frame for navigation. To be accordance with the navigation resolving output, the state equation and measurement equation shall be set up with the local horizontal coordinate system to be taken as the reference frame. The state equation shall be represented in matrix form as below:

$$\dot{X}(t) = F(t)X(t) + G(t)w(t), \tag{1}$$

where, $X(t)$ is state parameter vector, $F(t)$ is transfer matrix, $w(t)$ is white noise process at system state, $G(t)$ is noise drive matrix at system state. The tight integration state vector $X(t)$ shall be modeled to be

$$X(t) = [X_{IMU1} \ X_{IMU2} \ \delta L \ \delta \dot{L} \ \delta \rho_{GNSS1} \ \delta \dot{\rho}_{GNSS1} \ \delta \rho_{GNSS2} \ \delta \dot{\rho}_{GNSS2}]. \tag{2}$$

The parameters to be estimated shall include LINS systematic error X_{IMU_i} , flexure error δL , flexure change rate error $\delta \dot{L}$ varying with time, pseudo-range deviation $\delta \rho_{GNSS_i}$ corresponding to receiver clock error, and pseudo-

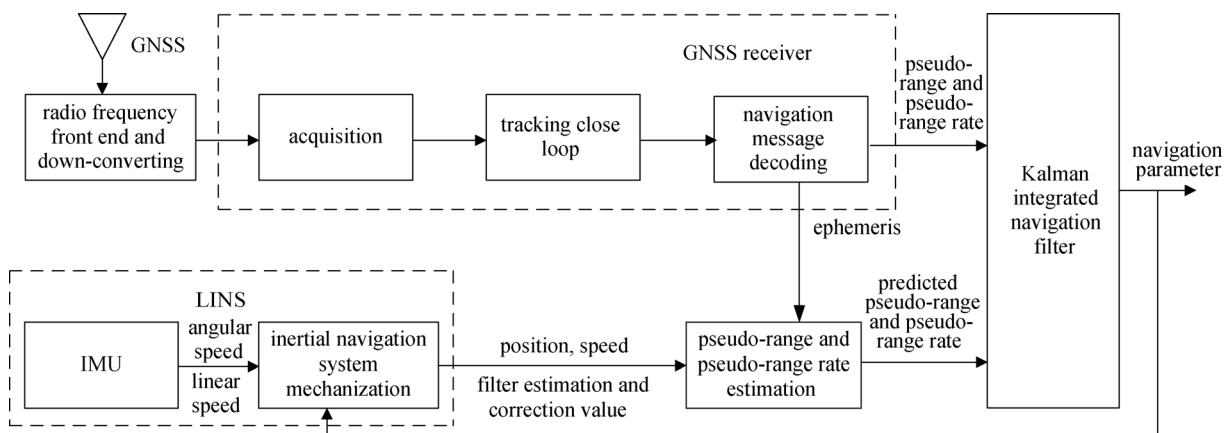


Fig. 2 Block diagram of tight integration GNSS/LINS

range rate deviation $\delta\dot{\rho}_{\text{GNSS}i}$ corresponding to receiver clock drift.

The state parameters related to LINS systematic error shall include: attitude error, velocity error, position error, gyroscope drift and acceleration bias, and there is an equation as below:

$$\mathbf{X}_{\text{IMU}i} = [\boldsymbol{\Psi} \quad \delta V \quad \delta \mathbf{p} \quad \mathbf{b}_g \quad \mathbf{b}_a]. \quad (3)$$

According to the state vectors to be estimated by LINS, the system state equations can be deduced according to the LINS error model, including the position error equation, velocity error equation and attitude error equation.

1) Position error equation [11,12]

The perturbation equation of position error shall be represented in vector as below:

$$\delta\dot{\mathbf{p}}_b = \delta\mathbf{v}_{nb}^n - [\boldsymbol{\omega}_{en}^n \times] \delta\mathbf{p}_b + [\delta\boldsymbol{\theta} \times] \mathbf{v}_{nb}^n, \quad (4)$$

where, $\delta\boldsymbol{\theta}$ is position error angular vector, $\delta\mathbf{v}_{nb}^n$ is velocity error vector in local horizontal coordinate, $\delta\mathbf{p}_b$ position error vector in latitude, longitude and altitude, i.e., $\delta\phi$, $\delta\lambda$, δh .

The position error equation shall be

$$\delta\dot{\mathbf{p}}_b = \mathbf{F}_{pp} \delta\mathbf{p}_b + \mathbf{F}_{pv} \delta\mathbf{v}_{nb}^n. \quad (5)$$

2) Velocity error equation

The perturbation equation of velocity error shall be represented in vector [11,12] as below:

$$\begin{aligned} \delta\dot{\mathbf{v}}_{nb}^n = & -\delta(\boldsymbol{\Omega}_{ie}^n + \boldsymbol{\Omega}_{in}^n) \mathbf{v}_{nb}^n + (\boldsymbol{\Omega}_{ie}^n + \boldsymbol{\Omega}_{in}^n) \delta\mathbf{v}_{nb}^n + \delta\mathbf{f}^n \\ & + \boldsymbol{\Gamma} \delta\mathbf{p}_b + \delta\mathbf{g}^n, \end{aligned} \quad (6)$$

where, $\delta\mathbf{f}^n$ is the projection of specific force in the local horizontal coordinate, $\boldsymbol{\Gamma}$ is normal gravitation calculation error coefficient matrix caused by the position error, $\delta\mathbf{g}^n$ is gravitational acceleration error vector in local horizontal coordinate.

The velocity error equation shall be represented as

$$\delta\dot{\mathbf{v}}_{nb}^n = \mathbf{F}_{vp} \delta\mathbf{p}_b + \mathbf{F}_{vv} \delta\mathbf{v}_{nb}^n + (\mathbf{f}^n \times) \boldsymbol{\Psi}_{nb}^n + \mathbf{C}_b^n \mathbf{b}_a. \quad (7)$$

3) Attitude error equation

The perturbation equation of attitude error shall be represented in vector [11,12] as below:

$$\dot{\boldsymbol{\Psi}}_{nb}^n = -[\boldsymbol{\omega}_{in}^n \times] \boldsymbol{\Psi}_{nb}^n + \delta\boldsymbol{\omega}_{in}^n - \mathbf{C}_b^n \delta\boldsymbol{\omega}_{ib}^b. \quad (8)$$

And the attitude error equation shall be

$$\dot{\boldsymbol{\Psi}}_{nb}^n = \mathbf{F}_{ep} \delta\mathbf{p}_b + \mathbf{F}_{ev} \delta\mathbf{v}_{nb}^n - [\boldsymbol{\omega}_{in}^n \times] \boldsymbol{\Psi}_{nb}^n - \mathbf{C}_b^n \delta\boldsymbol{\omega}_{ib}^b. \quad (9)$$

4) IMU bias error equation

The IMU bias model of gyroscope and accelerometer shall make use of the first-order Gauss-Markov process [13,14]

$$\begin{aligned} \dot{\mathbf{b}}_g &= -\frac{1}{T_{gb}} \mathbf{b}_g + \mathbf{w}_{gb}, \\ \dot{\mathbf{b}}_a &= -\frac{1}{T_{ab}} \mathbf{b}_a + \mathbf{w}_{ab}, \end{aligned} \quad (10)$$

where T_{gb} , T_{ab} are correlation time of gyroscope and accelerometer respectively corresponding to the first-order Gauss-Markov process, \mathbf{w}_{gb} , \mathbf{w}_{ab} are drive white noise corresponding to the first-order Gauss-Markov process.

5) Receiver clock error equation

The dynamic model of receiver clock error and drift shall be set up as

$$\begin{pmatrix} \delta\dot{\rho} \\ \delta\ddot{\rho} \end{pmatrix} = \begin{pmatrix} 0 & 1 \\ 0 & 0 \end{pmatrix} \begin{pmatrix} \delta\rho \\ \delta\dot{\rho} \end{pmatrix} + \begin{pmatrix} w_{c\dot{\rho}t} \\ w_{c\ddot{\rho}t} \end{pmatrix}, \quad (11)$$

where $\delta\rho$, $\delta\dot{\rho}$ are respectively pseudo-range and pseudo-range rate corresponding to clock error and drift, $w_{c\dot{\rho}t}$, $w_{c\ddot{\rho}t}$ are noise vector.

Combine the error models above and obtain the state equation coefficient matrix to be

$$(\mathbf{F}_{\delta t \delta i})_{2 \times 2} = \begin{bmatrix} 1 & \Delta t \\ 0 & 1 \end{bmatrix}_{2 \times 2}.$$

6) Lever arm flexure error equation

The lever arm flexure and its dynamic model [1] shall be set up as

$$\delta\dot{\mathbf{L}} = \delta\dot{\mathbf{L}} + \mathbf{w}_{\text{flex}},$$

$$\delta\ddot{\mathbf{L}} = -\alpha\delta\mathbf{L} - 2\beta\delta\dot{\mathbf{L}} + (\alpha - 2\beta)\mathbf{w}_{\text{flex}}, \quad (12)$$

where \mathbf{w}_{flex} is lever arm noise vector, α , β are damping factors.

7) State equation noise

The systematic noise vector shall be modeled to be

$$\mathbf{w} = [\mathbf{w}_{\text{IMU}1} \quad \mathbf{w}_{\text{IMU}2} \quad \mathbf{w}_{\text{flex}} \quad w_{c\dot{\rho}1} \quad w_{c\dot{\rho}2} \quad w_{c\ddot{\rho}1} \quad w_{c\ddot{\rho}2}], \quad (13)$$

where the clock error shall correspond to pseudo-range change rate power spectral density (PSD) $S_{c\dot{\rho}t}$, $S_{c\dot{\rho}t} = \sigma_{c\dot{\rho}t}^2 / \tau$, where $\sigma_{c\dot{\rho}t}$ is the pseudo-range standard deviation corresponding to the clock error. As for Temperature Compensated Crystal Oscillator (TCXO) clock, generally $S_{c\dot{\rho}t} \approx 0.01 \text{ m/s}$, where the clock frequency drift shall correspond to pseudo-range rate change rate power spectral density (PSD) $S_{c\ddot{\rho}t}$, $S_{c\ddot{\rho}t} = \sigma_{c\ddot{\rho}t}^2 / \tau$, where $\sigma_{c\ddot{\rho}t}$ is pseudo-range rate standard deviation corresponding to clock drift. As for TCXO clock, generally $S_{c\ddot{\rho}t} \approx 0.04 \text{ m}^2/\text{s}^3$ [10,15].

2.3 Measurement model

2.3.1 Pseudo-range observation equation

As for tight integration GNSS/LINS, if it is assumed that the GNSS antenna position calculated by LINS is $(x_1 \ y_1 \ z_1)^T$ and the satellite position determined by the

satellite ephemeris is $(x_s \ y_s \ z_s)^T$, the pseudo-range ρ_1 in LINS position can be worked out. With the pseudo-range measured by the GNSS receiver to be denoted as ρ_G , the pseudo-range and pseudo-range rate difference between LINS and GNSS shall be observed and measured by the integrated LINS. As the LINS center and GNSS antenna phase center is non-coincidence, reduction of GNSS phase center to LINS center is required in the process of equation deduction. Only the pseudo-range observation equation is given below, and the pseudo-range rate is similar to the pseudo-range observation equation.

1) Pseudo-range observation vector

If j satellites are observed, the pseudo-range observation vector shall be

$$z_\rho = [\delta\rho_1 \ \delta\rho_2 \ \dots \ \delta\rho_j]^T, \quad (14)$$

where $\delta\rho_j$ is the difference between pseudo-range predicted by LINS and observed by GNSS receiver.

$$\delta\rho_j = \rho_{1j} - \rho_{Gj}, \quad (15)$$

In GNSS receiver observation vector, the satellite clock error, troposphere delay error, ionosphere delay error, earth rotation effect error shall be removed [13], and weight of observation noise shall be determined according to the elevation angle and SNR [11].

2) Pseudo-range observation equation coefficient matrix

First, the function relation between observation vector and position (x, y, z) error vector in Cartesian coordinate system shall be set up. Secondly, the relationship between position (x, y, z) error vector in Cartesian coordinate system and position error vector (ENU) shall be determined. Finally, the function relation between position error vector (ENU) and system state error vector shall be worked out, including lever arm compensation.

a) Error vector in Cartesian coordinate system

$$\delta\rho_j = \rho_{1j} - \rho_{Gj} = e_{j1}\delta x + e_{j2}\delta y + e_{j3}\delta z + c\delta t_u + v_{\rho j}, \quad (16)$$

where $v_{\rho j} = -[cV_{t_j}^e - (V_{ion})_j - (V_{trop})_j]$.

If j satellites are observed, Eq. (16) can be rewritten to be

$$z_\rho = A_\rho \delta r^e + I_\rho c\delta t_u + v_\rho, \quad (17)$$

where

$$z_\rho = [\delta\rho_1 \ \delta\rho_2 \ \dots \ \delta\rho_j]^T,$$

$$A_\rho = \begin{bmatrix} e_{11} & e_{12} & e_{13} \\ e_{21} & e_{22} & e_{23} \\ \vdots & \vdots & \vdots \\ e_{j1} & e_{j2} & e_{j3} \end{bmatrix},$$

$$\delta r^e = [\delta x \ \delta y \ \delta z]^T,$$

$$I_\rho = \text{diag}(1 \ 1 \ \dots \ 1),$$

$$v_\rho = [v_{\rho 1} \ v_{\rho 2} \ \dots \ v_{\rho j}]^T.$$

b) Error vector in local horizontal rectangular coordinate

$$\begin{bmatrix} \delta x \\ \delta y \\ \delta z \end{bmatrix} = C_n^e \begin{bmatrix} \delta r_E \\ \delta r_N \\ \delta r_U \end{bmatrix}. \quad (18)$$

c) Latitude, longitude and altitude error vector [12]

$$\begin{bmatrix} \delta r_E \\ \delta r_N \\ \delta r_U \end{bmatrix} = D_R \begin{bmatrix} \delta\phi \\ \delta\lambda \\ \delta h \end{bmatrix}$$

$$= \begin{bmatrix} 0 & (R_N + h)\cos\phi & 0 \\ R_M + h & 0 & 0 \\ 0 & 0 & 1 \end{bmatrix} \begin{bmatrix} \delta\phi \\ \delta\lambda \\ \delta h \end{bmatrix}. \quad (19)$$

d) IMU error vector with lever arm effect to be considered

If it is assumed that the GNSS antenna phase center is r_{GPS}^n in n system, IMU center is r_{IMU}^n in n system, the vector from GNSS antenna phase center to LINS center shall be l_{GPS}^b , and there is relationship as below.

$$r_{GPS}^n = r_{IMU}^n + D_R^{-1} C_b^n l_{GPS}^b, \quad (20)$$

where

$$D_R^{-1} = \begin{bmatrix} 0 & \frac{1}{R_M + h} & 0 \\ \frac{1}{(R_N + h)\cos\phi} & 0 & 0 \\ 0 & 0 & 1 \end{bmatrix}.$$

The calculated position of GNSS phase center can be written as

$$\hat{r}_{GPS}^n = r_{GPS}^n + \delta r_{IMU}^n + D_R^{-1} [C_b^n l_{GPS}^b \times] \phi. \quad (21)$$

From Eq. (21), it can be obtained that

$$\delta r_{GPS}^n \approx \delta r_{IMU}^n + D_R^{-1} [C_b^n l_{GPS}^b \times] \phi. \quad (22)$$

e) Composite derivation to be written in form of matrix

$$z_\rho = H_\rho x + v_\rho, \quad (23)$$

where

$$H_\rho = [(A_\rho C_n^e D_R C_1)_{j \times 3} \ \mathbf{0}_{j \times 3} \ (A_\rho C_n^e D_R)_{j \times 3} \ \mathbf{0}_{j \times 6} \ (I_\rho)_{j \times 1} \ \mathbf{0}_{j \times 1}]_{j \times 17} \quad (24)$$

and

$$C_1 = [C_b^n l_{GPS}^b \times]. \quad (25)$$

2.3.2 Carrier phase differential position vector observation equation

In the process of refreshing the carrier phase differential position, the resolved position vector difference between two LINSs shall be set to be

$$\mathbf{L}_{\text{INS}} = [dx_{\text{INS}} \quad dy_{\text{INS}} \quad dz_{\text{INS}}].$$

The position vector difference obtained by GNSS differential positioning shall be

$$\mathbf{L}_{\text{GNSS}} = [dx_{\text{GNSS}} \quad dy_{\text{GNSS}} \quad dz_{\text{GNSS}}].$$

The observation vector $\Delta\mathbf{L}_{\text{GNSS}} = [\mathbf{L}_{\text{INS}} - \mathbf{L}_{\text{GNSS}}]$ can be used to construct a differential position vector observation equation as below, where \mathbf{H} is the coefficient matrix.

$$\Delta\mathbf{L}_{\text{GNSS}} = \mathbf{H}\mathbf{X}. \quad (26)$$

3 Experiment and discussion

A turntable is used to simulate the hull flexure to estimate the accuracy of hull flexure measurement method proposed in this paper. In the place where receiver antenna can receive the signal of satellites, two sets of measurement units of integrated GNSS/LINS shall be installed fixedly at the two end of long test tooling showed in Fig. 3 respectively. The two devices are 3 meters apart.

Before testing, the angular output of swing table and output of integrated GNSS/LINS measurement units shall be calibrated to be temporally and angularly synchronized.

After the swing table is settled down (about 5 min after starting), it shall keep swinging in 5° amplitude and 10 s cycle for totally 2 h. Note down the angular output.

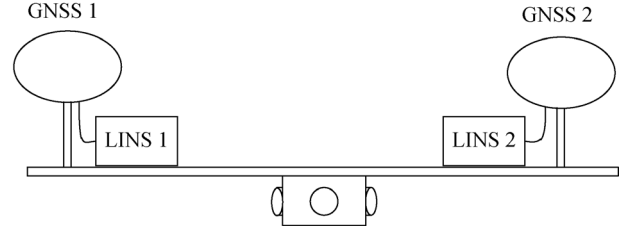


Fig. 3 Experimental set-up of GNSS/LINS

3D position variation shall be resolved according to the fixed baseline length of the testing bench and the attitude output of swing table, which shall be taken as a reference value to compare with the 3D flexure measured by the integrated GNSS/LINS measurement unit. The measured displacement flexure error in east, north and up direction respectively resolved by GNSS and integrated GNSS/LINS are shown in Figs. 4–6. Wherein, the displacement flexure error resolved by GNSS is represented by the red curve, while resolved by integrated GNSS/LINS by the blue curve.

It is known from the figures above that the flexure measurement noise of GNSS is significantly larger than integrated GNSS/LINS measurement results. At the same time, it can be found that during the period of 5500 to 5700 s, the measurement results of GNSS occur in all three directions with the maximal measurement error reaches 0.12 m. During this period, the maximal flexure measurement error of integrated GNSS/LINS is lower than 0.04 m. It is shown by analyzing the carrier phase differential positioning data of GNSS that the integer ambiguity during the above period cannot be fixed and the output is a floating point solution. From Figs. 7 and 8, it can be found

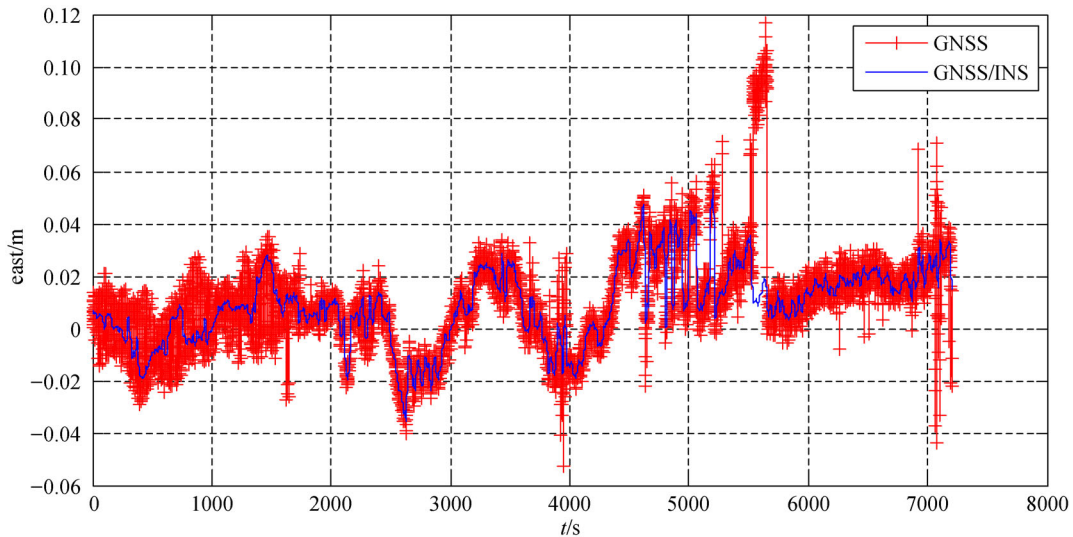


Fig. 4 Flexure measurement error in east direction

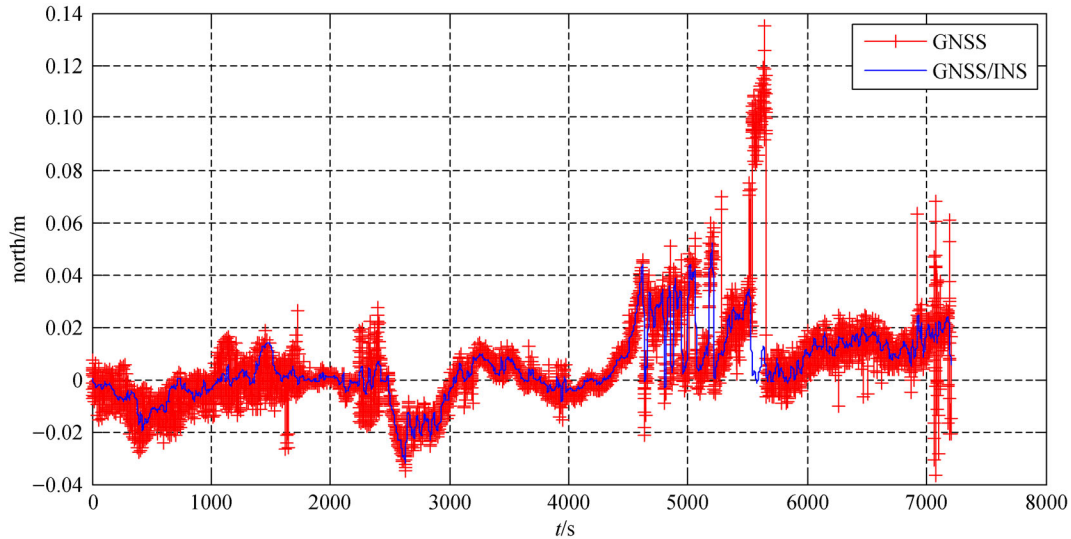


Fig. 5 Flexure measurement error in north direction

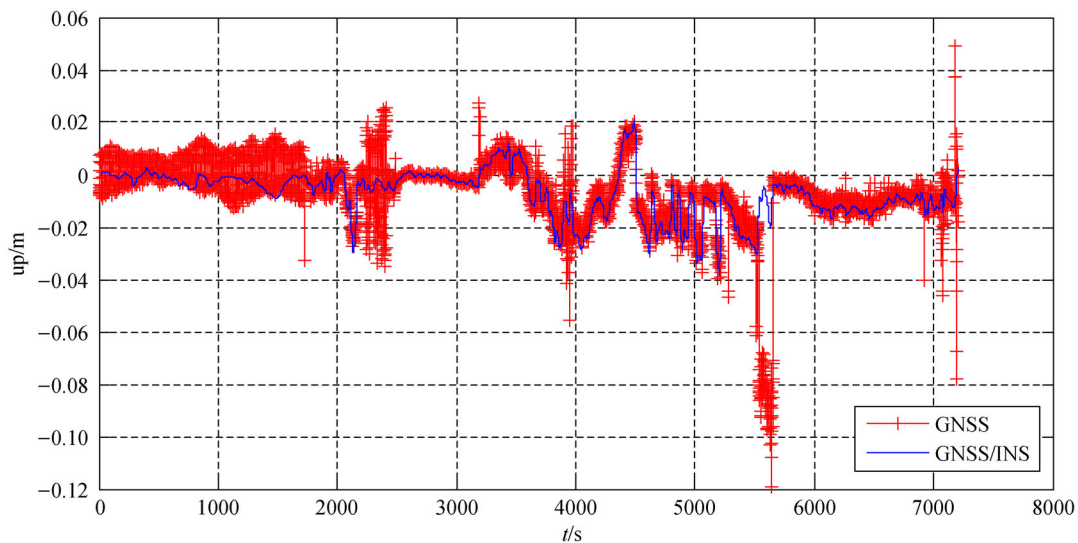


Fig. 6 Flexure measurement error in up direction

that the number of differential common-view satellites is greatly reduced during the above period and the horizontal dilution of precision (HDOP) is significantly increased; therefore, the major GNSS positioning error may probably be caused by external environment factors, such as satellite signal obstruction and multi-path effect error causes cycle slip [16,17] that resulting in unfixed integer ambiguity and consequently big measurement error.

GNSS/LINS integration measurement can effectively detect and eliminate satellite navigation measurement deviation by using high-precision laser gyro measurement information for information fusion, which ensures low-noise and high-precision measurement characteristics in a short time during flexure measurement. According to

statistics, the estimation error (1σ) of the flexure components in the east, north and up directions of the laser gyro inertial/satellite combination is 0.0169, 0.0128 and 0.0115 m, respectively.

Since the laser inertial position accuracy diverges with time, when only the laser inertial conduction is used for the flexure measurement, only the accurate flexure angle measurement can be realized, and the flexure position cannot be accurately measured. For the hull flexure, the same flexure angle error is obtained. If the baseline is too long, it will cause a larger positional flexure error, and the flexure error measured by this method is independent of the baseline length, which is more suitable for shipboard guided navigation.

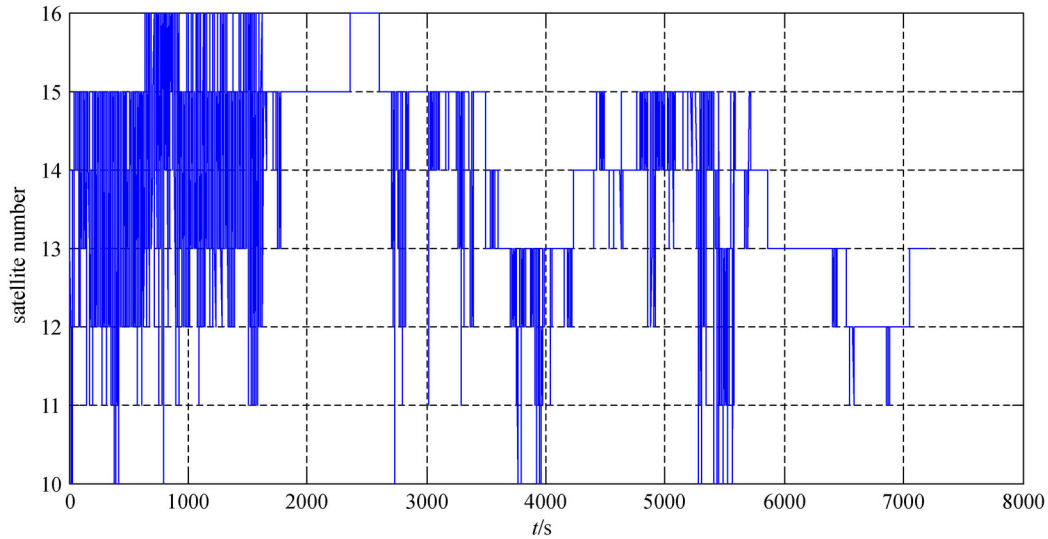


Fig. 7 Number of common-view satellites for differential positioning

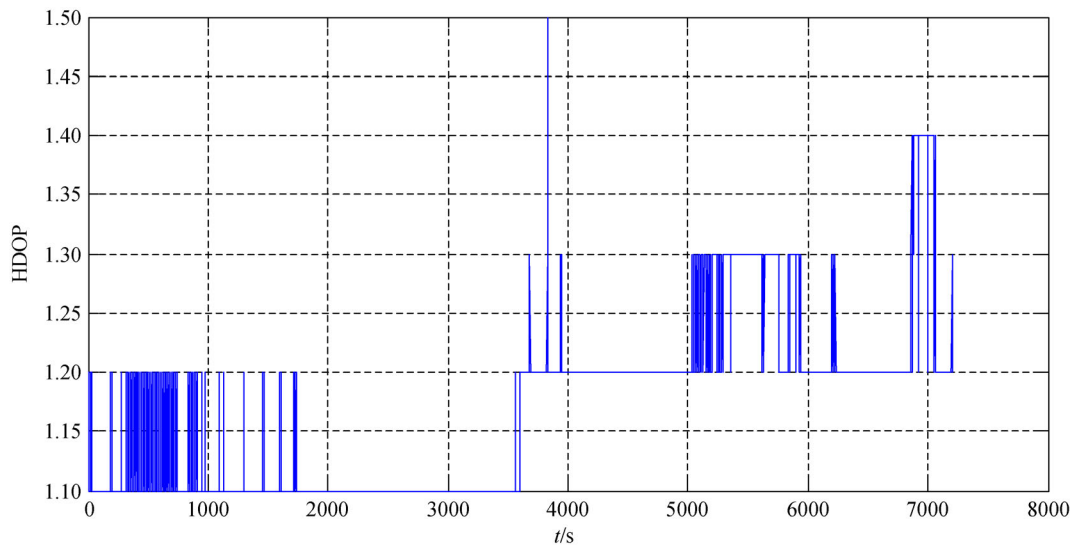


Fig. 8 HDOP for GNSS differential positioning

4 Conclusion

To meet the requirement of hull flexure measurement, an integrated GNSS/LINS measurement method is proposed for high accuracy flexure monitoring. The conceptual design and operation principle are presented. A high-order Kalman filter GNSS/LINS estimation model is established. Through the simulation analysis of the hull flexure by the turntable, it is verified that the hull flexure measurement accuracy based on the inertial/satellite combination is better than 0.02 m, which can effectively overcome the measurement error caused by the external navigation of satellite navigation. Meanwhile, the accuracy of the methodology used in this paper is independent with the length of the baseline, which is more suitable for carrier

aircraft landing guidance by comparing with other methods.

References

1. Feng T, Mao X. Multimodal data fusion for SRGPS antenna motion error reduction. *Multimedia Tools and Applications*, 2017, 76(9): 12035–12050
2. IS A, Ray B. Development and evaluation of a precision coordinate transfer system for SRGPS. In: *Proceedings of International Technical Meeting of the Satellite Division of the Institute of Navigation*, 2004
3. Wang J, Zhang G. Two-frequency polarization method for metering of instrumentation ship's hull transverse twist. *Optics and Precision*

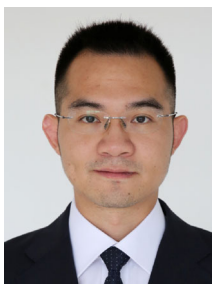
- Engineering, 1999, 7(3): 118–123
4. Zhang Y, Li M, Yu P. Research on angle diatortion for the measuring ship. *Chinese Journal of Scientific Instrument*, 2006, 27(6): 1505–1507
 5. Li Y, Zhang Y, Yue J. New technology of ship distortion measurement. *Optics and Precision Engineering*, 2008, 16(11): 2235–2238
 6. Sun C, Liu H, Chen S, Zhang X. Semi-physical simulation experimental study of hull vertical deformation measurement based on videometrics principle. *Journal of Experimental Mechanics*, 2015, 30(5): 599–606
 7. Petovello M G, Lachapelle G, Cannon M E. Using GPS and GPS/INS systems to assess relative antenna motion onboard an aircraft carrier for shipboard relative GPS. In: *Proceedings of International Technical Meeting of the Institute of Navigation*, 2005, 219–229
 8. Yuan E, Yang G, Yu P, Tang G. Transfer method of ship's attitude references based on inertial matching method. *Ship Science and Technology*, 2013, 35(12): 60–64
 9. Zhang Y, Li M, Yu P. Research on angle distortion for the measuring ship. *Chinese Journal of Scientific Instrument*, 2006, 27(6): 1505–1507
 10. Chen Q J. *Research on the Railway Track Geometry Surveying Technology Based on Aided INS*. Wuhan: Wuhan University, 2016
 11. Groves P D. *Principles of GNSS, Inertial, and Multisensor Integrated Navigation Systems*. Boston: Artech House, 2013
 12. Farrell J A. *Aided Navigation GPS with High Rate Sensor*. New York: The McGraw-Hill Companies, 2008
 13. Dong X R, Zhang S X. *GPS/INS Integrated Navigation and Its Application*. Changsha: National Defense Science and Technology University Press, 1998
 14. Sun H X. *DGPS/INS Integrated Position and Attitude Determination and Its Application in MMS*. Wuhan: Wuhan University, 2004
 15. Brown G, Robert, Patrick Y C. *Introduction to Random Signals and Applied Kalman Filtering*. Vol. 1, No. 1. New York: John Wiley & Sons, 1992
 16. Li Z H, Huang J S. *GPS Surveying and Data Processing*. Wuhan: Wuhan University Press, 2010
 17. Ning Y P, Wang J, Hu X X, Wang S D. Inertial aided cycle-slip detection and repair for BDS triple-frequency signal in severe multipath environment. *Acta Geodaetica et Cartographica Sinica*, 2016, 45(S2): 179–187



Di Wu is a doctor at the National Space Science Center, Chinese Academy of Sciences. She got the master degree from Beijing Institute of Technology in 2009. Her current fields of interests include digital signal processing of GNSS radio remote sensing, GNSS-R remote sensing techniques, embedded system design, software system design of satellite receiver.



Yu Jia is a senior engineer of Huazhong Institute of Electro-optics—Wuhan National Laboratory for Optoelectronics. He got the master degree from Southwest Jiaotong University in 2005. His current research fields include electro-optical system, laser gyro inertial navigation, multi-sensor navigation information fusion software design, etc.



Li Wang is a senior engineer of Huazhong Institute of Electro-optics—Wuhan National Laboratory for Optoelectronics. He got the doctor degree from Wuhan University in 2015. His current research fields include laser gyro inertial navigation, satellite navigation, multi-sensor navigation information fusion hardware design, etc.



Yueqiang Sun is a professor at the National Space Science Center, Chinese Academy of Sciences. Prof. Sun got her doctor degree from National Space Science Center, Chinese Academy of Sciences, in 2002. She devotes to develop GNSS remote sensing and space-borne special environment exploration technologies. She has been the principal investigator or vice principal investigator of more than twenty missions/projects in manned space flight, FengYun and 863 Project. Her interested research areas include GNSS radio occultation, GNSS-R remote sensing techniques, atmospheric physics, ionospheric physics, magnetic physics, space physics, and so on.